Tunable Plasmonic Nanostructures: from Fundamental Nanoscale Optics to Surface-enhanced Spectroscopies

Hui Wang

Department of Chemistry, Rice University, Houston, Texas, 77005, USA

The fascinating optical properties of metallic nanostructures, dominated by collective oscillations of free electrons known as plasmons, open new opportunities for the development of fundamentally new metal-based subwavelength optical elements with broad technological potential.[1-5] This thesis demonstrates the rational design and controllable fabrication of a whole family of novel plasmonic nanostructures with geometrically tunable optical properties with a particular focus on utilizing plasmonic nanostructures to optimize molecular sensing platforms based on surface-enhanced spectroscopies.

Tunable Plasmons of Metallic Nanoshells

The starting point of this thesis is metallic nanoshell which is composed of a spherical dielectric core surrounded by a concentric metallic thin shell. The plasmon resonant frequencies of a nanoshell can be fine-tuned across the visible and near-infrared regions of the spectrum by tailoring the core-shell dimensions (Figure 1A). Plasmon Hybridization theory,[6, 7] a mesoscale electromagnetic analog of molecular orbital theory, has been developed to theoretically calculate the nanoshell plasmons. In the context of this conceptually enlightening model, the nanoshell plasmon resonances essentially result from the interaction between plasmon response of a sphere and that of a cavity (Figure 1B).[7]

Au nanoshells can be fabricated by seed-mediated electroless plating method.[8] Here we have developed an improved protocol for the fabrication of nearly perfect Au nanoshells with precisely controlled core-shell dimensions (Figure 1C).[9] The high quality of the as-fabricated nanoshells enables excellent agreement between measured extinction spectra and Mie theory calculations (Figure 1D). In addition to core-shell dimensions, the optical properties of a nanoshell are also determined by the electronic structures of the constituent metals. Strikingly different from Au and Ag nanoshells, strong interband transitions of Cu overlaps the plasmonic response of Cu nanoshells in the visible region, resulting in unique double-peaked plasmon resonances.[10]

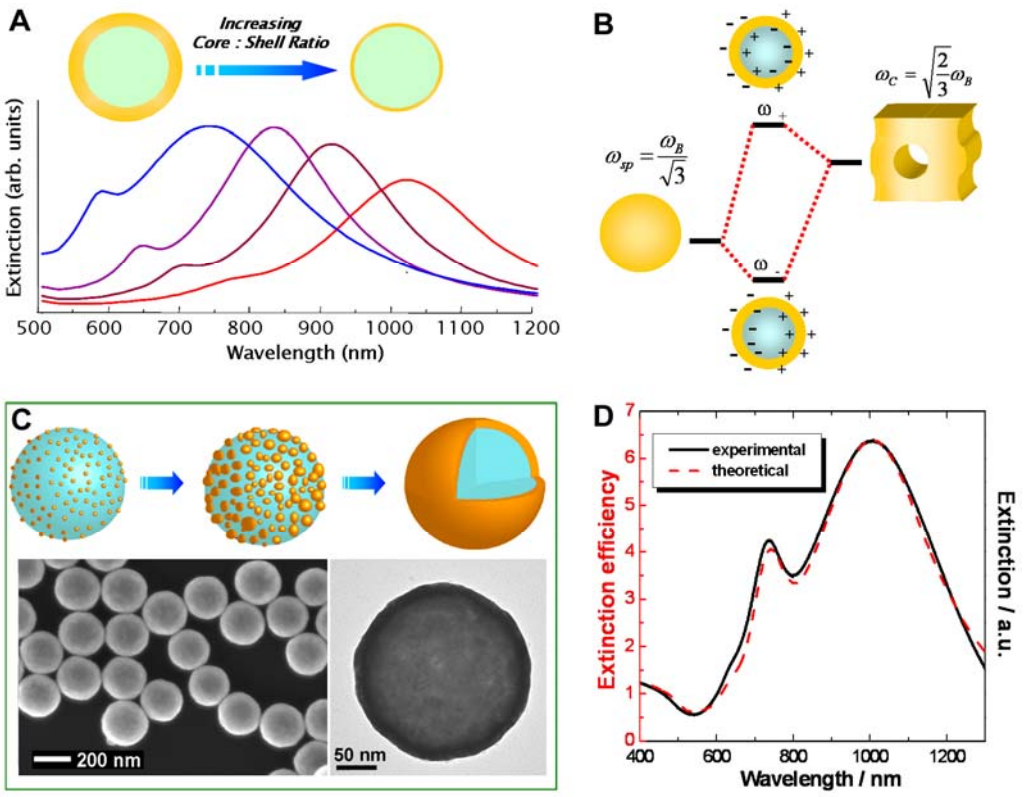

Figure 1 (A) Plasmonic tunability demonstrated for Au nanoshells with core (silica) radius of 60 nm and shell thickness of 5, 10, 15, and 20 nm. (B) Energy level diagram depicting plasmon hybridization in metal nanoshells resulting from interacting sphere and cavity plasmons. The two hybridized plasmon modes are an anti-bonding plasmon (ω_+) and a bonding plasmon resonance (ω_-). (C) Cartoon illustration of nanoshell fabrication and SEM and TEM images of experimentally fabricated nanoshells. (D) Experimentally measured (black solid curves) and theoretically calculated (red dash curves) extinction spectra of nanoshells with core radius of 91 $\pm$ 6 nm and shell thickness of 10 $\pm$ 1 nm.

Symmetry-breaking of Individual Plasmonic Nanoparticles

We have systematically investigated how symmetry-breaking modifies the plasmonic properties of individual nanoparticles and introduces improved optical characteristics directly relevant to sensing applications. Our starting point here is still the concentric nanoshells, and we break the symmetry of a nanoshell in different ways to fabricate two brand-new plasmonic nanostructures with reduced symmetry: prolate nanoshells known as nanorice and nanoshells with an offset core known as nanoeggs.

Nanorice is a new hybrid nanoparticle geometry that combines the intense local fields of nanorods with the highly tunable plasmon resonances of nanoshells (Figure 2).[11] The highly tunable nanorice plasmons essentially arise from plasmon hybridization between a metallic spheroid and an ellipsoidal nanocavity. The excitation of the longitudinal nanorice plasmon gives rise to enormous local field enhancements exploitable for surface-enhanced Raman spectroscopy (SERS). The longitudinal plasmon resonance frequency of nanorice is extremely sensitive to surrounding dielectric media, holding great potential for monitoring localized environmental changes during chemical and biological processes.

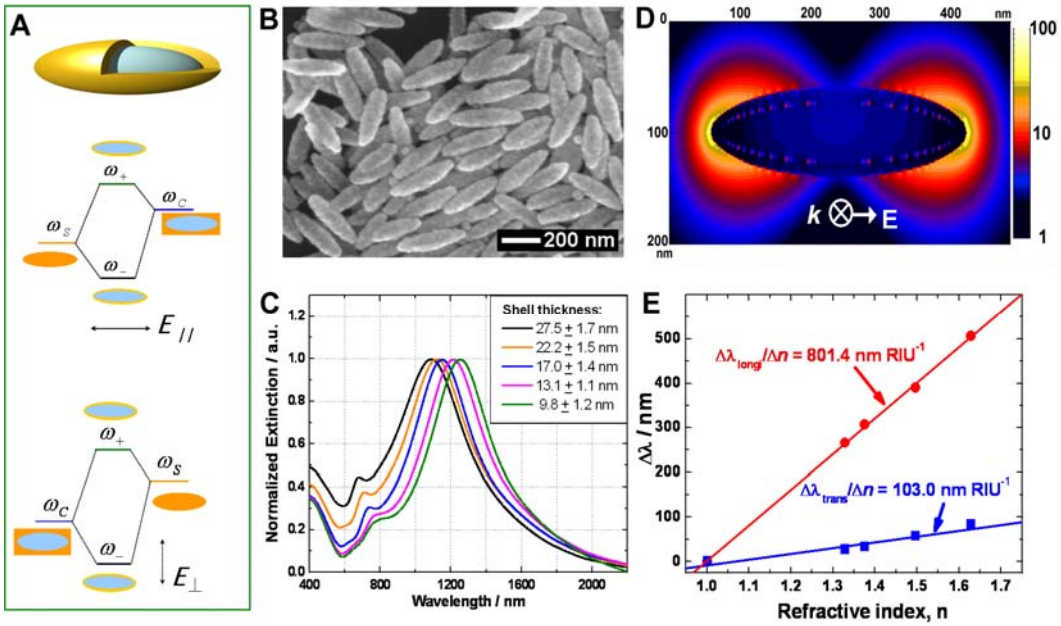

Figure 2 (A) Cartoon illustration of nanorice geometry (top) and plasmon hybridization of nanorice for longitudinal (middle) and transverse (bottom) modes. (B) SEM image of nanorice. (C) Extinction spectra of nanorice with different shell thicknesses. (D) Calculated near-field contour of a nanorice particle excited at longitudinal plasmon resonant frequency using Finite-Difference Time Domain method (FDTD). (E) Shift of longitudinal and transverse plasmon energies as function of the refractive index of surrounding media.

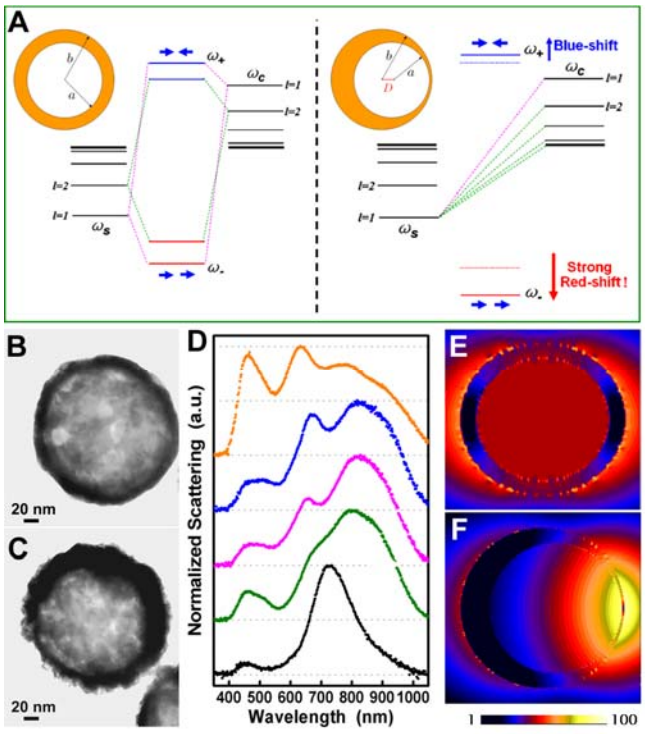

Figure 3 (A) Schematic of plasmon hybridization in a concentric nanoshell (left) and a non-concentric nanoshell, or nanoegg (right). (B) TEM image of a nanoshell. (C) TEM image of a nanoegg. (D) Normalized single particle dark-field scattering spectra of a nanoshell (black curve, [*a*, *b*] = [94, 103] nm.) and four different nanoegg particles (colored spectra). Nanoeggs were fabricated by electroless plating of Au onto the exposed surfaces of deposited nanoshells, to a maximum core offset of ~ 16 nm. Calculated near-field plots of (E) a nanoshell ([*a*, *b*]=[39, 48] nm) and (F) a nanoegg ([*a*, *b*, *D*]=[39, 48, 7.5] nm The incident field is horizontally polarized.

The introduction of an off-center core inside a metallic shell radically changes optical responses of the nanoparticle due to the relaxation of selection rules of plasmon hybridization (Figure 3A).[12] For a spherically concentric nanoshell, plasmon hybridization only occurs between cavity and sphere plasmon modes of the same angular momentum. However, when the center of the inner core is displaced with respect to the center of the outer shell, cavity and sphere plasmons of all multipolar indices mix and contribute to the bonding and antibonding plasmon modes of nanoeggs. The experimentally obtained optical spectra of the individual nanoparticles clearly show the characteristic offset-dependent multiple-peak feature (Figure 3D). Nanoeggs also exhibit greatly improved near-field properties exploitable for surface-enhanced spectroscopies compared to concentric nanoshells (Figures 3E and F).

Nanoscale Surface Texturing of Subwavelength Metallic Particles

Roughened subwavelength particles are of great interest in light scattering studies, since a wide variety of naturally occurring particles, such as biological structures or atmospheric dust, have surfaces with nanoscale roughness. For roughened metallic particles, the enhanced local-field is one mechanism that predominantly contributes to the signal strength in surface-enhanced spectroscopies. Here we have developed two facile and controllable chemical methods for nanoscale surface texturing of Au nanoshells.[13, 14] We have systematically investigated how nanoscale surface roughness introduces dramatic changes to the optical properties of nanoshells including far-field extinction, near-field enhancements, and special distribution of scattering light (Figure 4). We discovered that for roughened Au particles in mesoscopic size regime, higher-order multipole modes, such as quadrupole, octople and hexadecapole resonances, are considerably quenched by the nanoscale surface roughness.[14, 15] Nanoscale roughness also significantly increases local field enhancements on the surface of these mesoscopic particles, achieving 10^6-10^7 SERS enhancements on individual particles.[15]

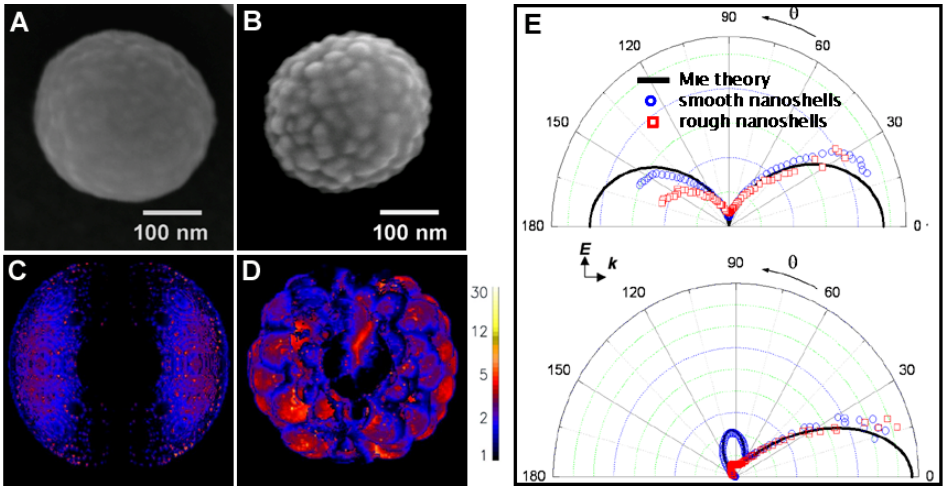

Figure 4 SEM images of (A) a smooth nanoshell and (B) roughened nanoshell. Near-field plots of (C) a smooth nanoshell and (D) roughened nanoshell simulated using 3D-FDTD method. (E) Angle-dependent light scattering from smooth and roughened nanoshell antennas illuminated at dipole resonance (top) and quadrupole resonance (bottom).

Hybridized Plasmons in Multinanoparticle Systems

An important topic in nanophotonics is how the plasmon modes of a nanoparticle change in close proximity to other nanoparticles. We have constructed a series of multinanoparticle systems utilizing Au nanospheres or nanoshells as the building blocks. Plasmon Hybridization model allows us to express the fundamental plasmon modes of these multiparticle systems as linear combinations of individual nanoparticle plasmons.

The simplest multinanoparticle system is a pair of directly adjacent, interacting nanoparticles known as a dimer. A novel fabrication and positioning approach has been developed for the stepwise assembly of upright nanoshell heterodimers in a semi-embedded geometry, and the asymmetric plasmon hybridization of the heterodimer has been clearly observed (Figure 5).[16]

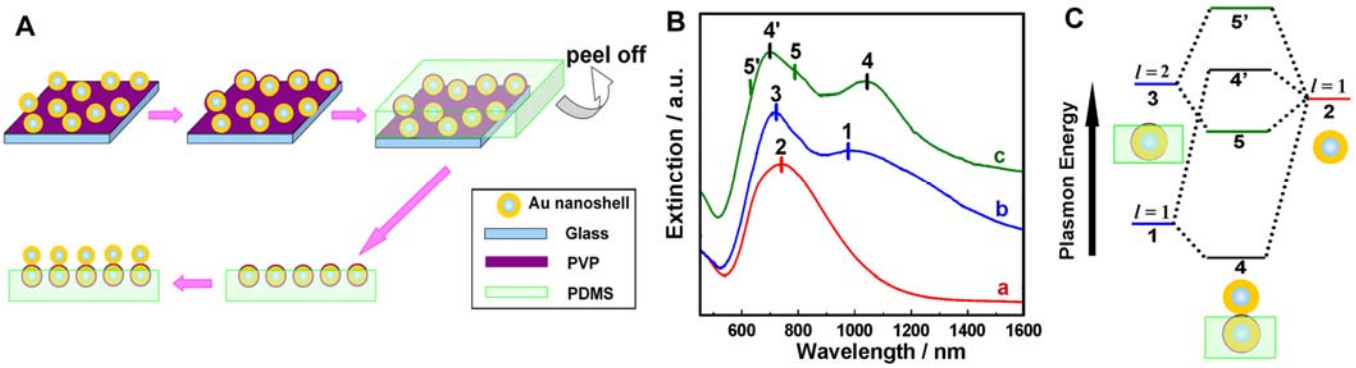

Figure 5 (A) Cartoon illustration of nanoshell heterodimer fabrication. (B) Extinction spectra of (a) nanoshells on glass slide exposed in air, (b) nanoshells partially embedded in PDMS, and (c) nanoshell heterodimers. (C) Energy diagram showing the schematics of how the plasmon modes of two individual nanoshells hybridize to form dimer plasmon modes.

We have also developed a convenient and cost-effective chemical self-assembly approach to highly ordered Au nanosphere arrays with sub-10 nm interparticle spacing (Figures 6A-D).[17] These sub-10 nm gaps between adjacent nanoparticles have been proven to be crucial for large SERS enhancements.[17] We have further developed a specifically designed, subwavelength-structured metallic substrate that simultaneously enhances two complementary vibrational spectroscopies, Raman scattering and Infrared absorption, by introducing plasmon resonances at the two diverse frequency regions required for both spectroscopies.[18] Our strategy is based on self-assembly of near-infrared resonant nanoshells into 2D periodic arrays with sub-10 nm interparticle gaps. The resulting nanoshell array is a unique structure which possesses hot spots in the interparticle junctions that enhance Raman scattering by a factor of 10^8-10^9 at near-infrared wavelengths, and simultaneously provide broadband mid-infrared hot spots that enhance Infrared absorption by a factor of 10^4 on the same substrates.

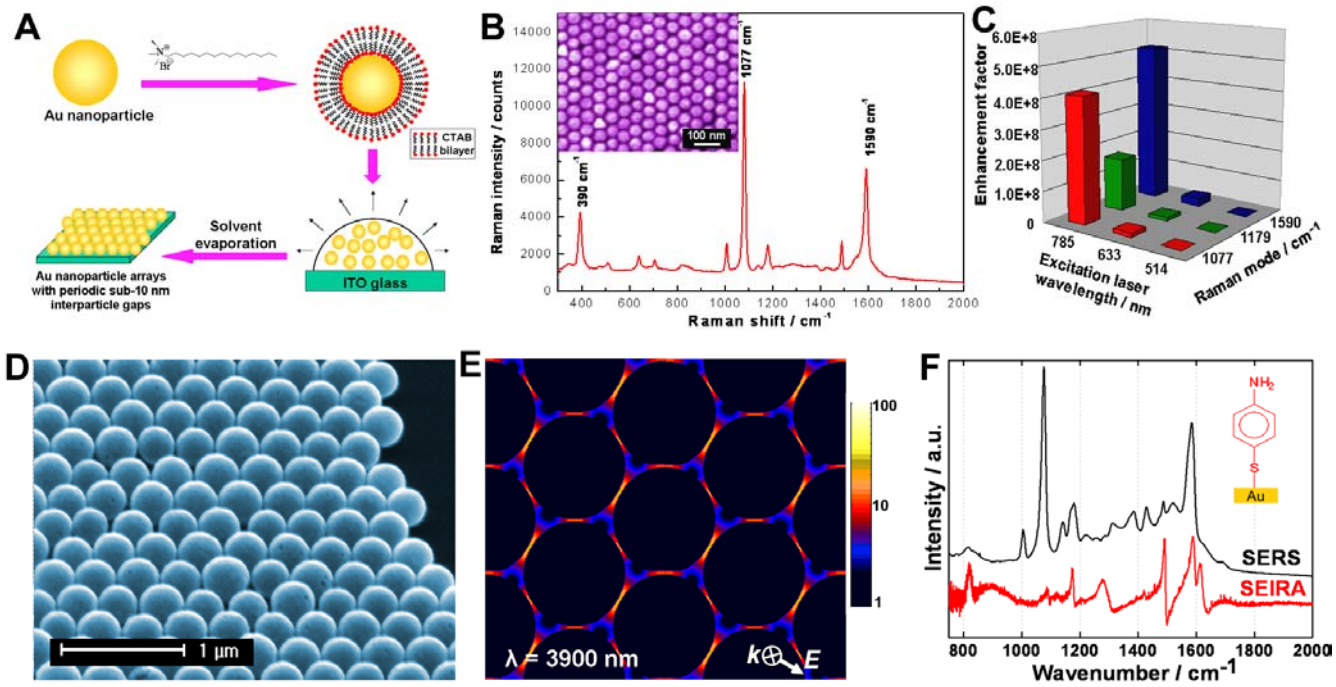

Figure 6 (A) Cartoon illustration of the fabrication of Au nanosphere arrays with sub-10 nm interparticle gaps. (B) SERS spectrum of *para*-mercaptoaniline on the Au nanosphere arrays. (Inset: SEM image of Au nanosphere arrays). (C) SERS enhancement factors of *para*-mercaptoaniline on the Au nanosphere arrays. (D) SEM image of nanoshell arrays. (E) FDTD-calculated near-field plots of nanoshell arrays under mid-infrared excitation. (F) SERS and SEIRA spectra of *para*-mercaptoaniline on nanoshell arrays.

Summary

In summary, this thesis covers four important aspects: 1) design of new plasmonic nanostructures driven by functions; 2) development of new strategies to fabricate and assemble functional plasmonic nanostructures; 3) understanding the properties of these optically active nanosystems; 4) utilizing plasmonic nanostructures to optimize molecular sensing processes. Plasmon hybridization model is the core of our design principle, providing a simple but extremely powerful way to gain deep insight into the relationship between nanoparticle geometry and resulting optical properties. The nanoparticle fabrication and assembly strategies we have developed provide important means to experimentally realize the nanoparticle geometries through which the desired properties and functionalities can be achieved. The development of multifunctional ultrasensitive molecular sensing platforms based on surface-enhanced spectroscopies demonstrates how optimized optical properties and functionalities can be selectively implemented into structures and devices of nanoscale dimensions for specific applications.

References:

1. Barnes, W. L.; Dereux, A.; Ebbesen, T. W. *Nature* **2003,** 424, 824-830.
2. Maier, S. A.; Brongersma, M. L.; Kik, P. G.; Meltzer, S.; Requicha, A. A. G.; Atwater, H. A. *Adv. Mater.* **2001,** 13, 1501-1505.
3. Ozbay, E. *Science* **2006,** 311, 189-193.
4. Xia, Y.; Halas, N. *MRS Bulletin* **2005,** 30, 338-344.
5. Nie, S.; Emory, S. R. *Science* **1997,** 275, (5303), 1102-1106.
6. Prodan, E.; Radloff, C.; Halas, N. J.; Nordlander, P. *Science* **2003,** 302, 419-422.
7. Wang, H.; Brandl, D. W.; Nordlander, P.; Halas, N. J. *Acc. Chem. Res.* **2007,** 40, 53-62.
8. Oldenburg, S. J.; Averitt, R. D.; Westcott, S. L.; Halas, N. J. *Chem. Phys. Lett.* **1998,** 288, (2-4), 243-247.
9. Wang, H.; Halas, N. J.*, manuscript in preparation for submission*.
10. Wang, H.; Tam, F.; Grady, N. K.; Halas, N. J. *J. Phys. Chem. B* **2005,** 109, 18218-18222.
11. Wang, H.; Brandl, D. W.; Le, F.; Nordlander, P.; Halas, N. J. *Nano Lett.* **2006,** 6, 827-832.
12. Wang, H.; Wu, Y.; Lassiter, B.; Nehl, C. L.; Hafner, J. H.; Nordlander, P.; Halas, N. J. *Proc. Natl. Acad. Sci. USA* **2006,** 103, 10856-10860.
13. Wang, H.; Goodrich, G. P.; Tam, F.; Oubre, C.; Nordlander, P.; Halas, N. J. *J. Phys. Chem. B* **2005,** 109, 11083-11087.
14. Wang, H.; Fu, K.; Drezek, R. A.; Halas, N. J. *Appl. Phys. B* **2006,** 84, 191-195.
15. Wang, H.; Halas, N. J. *Adv. Mater.* **2008,** in press.
16. Wang, H.; Halas, N. J. *Nano Lett.* **2006,** 6, 2945-2948.
17. Wang, H.; Levin, C. S.; Halas, N. J. *J. Am. Chem. Soc.* **2005,** 127, 14992-14993.
18. Wang, H.; Kundu, J.; Halas, N. J. *Angew. Chem. Int. Ed.* **2007,** 46, 9040-9044.